# Specific elimination of mutant mitochondrial genomes in patient-derived cells by mitoTALENs

Sandra R Bacman[1,3], Siôn L Williams[1,3], Milena Pinto[1], Susana Peralta[1] & Carlos T Moraes[1,2]

**Mitochondrial diseases are commonly caused by mutated mitochondrial DNA (mtDNA), which in most cases coexists with wild-type mtDNA, resulting in mtDNA heteroplasmy. We have engineered transcription activator-like effector nucleases (TALENs) to localize to mitochondria and cleave different classes of pathogenic mtDNA mutations. Mitochondria-targeted TALEN (mitoTALEN) expression led to permanent reductions in deletion or point-mutant mtDNA in patient-derived cells, raising the possibility that these mitochondrial nucleases can be therapeutic for some mitochondrial diseases.**

Most often, pathogenic mtDNA mutations are heteroplasmic, and residual wild-type mtDNA can partially compensate for the mutated mtDNA[1–3], averting a bioenergetic crisis. However, when the ratio of mutant mtDNA to wild-type mtDNA exceeds approximately 4:1, biochemical and clinical manifestations can result[1]. Therefore, several approaches have been tried to selectively reduce the levels of mutant mtDNA while sparing wild-type mtDNA to skew this ratio back to a healthier range[4–6]. However, previous attempts have been ineffective in living cells and have lacked the flexibility to target clinically relevant mutations, did not produce stable changes in heteroplasmy or were not readily translatable to animals.

The use of mitochondria-targeted nucleases showed some promise in their ability to alter mtDNA heteroplasmy in living cells[4,7]. To expand their use, we re-engineered TALENs[8,9] as a potentially flexible platform to reduce the abundance of mutated mtDNA relative to wild-type mtDNA. We tested this approach by designing a mitoTALEN to cleave the breakpoint region of an mtDNA with a large 5-kilobase deletion, m.8483_13459del4977. This mutation is known as the 'common deletion' because it is present in approximately 30% of all patients with mtDNA deletions[10], as well as in normal aging tissues[11,12]. We exploited the dimerization requirement of TALENs and designed the mitoTALEN for eliminating the common deletion (Δ5-mitoTALEN) so that each monomer binds a specific wild-type sequence flanking the region to be removed. Only when bound to deletion-mutant mtDNA are the Δ5-mitoTALEN monomers close enough to promote FokI dimerization and cleavage (**Fig. 1a**).

BLAST analysis did not detect perfect homology of the selected target region in the nuclear genome (**Supplementary Table 1**).

We made a series of modifications to rationally design mitoTALENs (**Fig. 1b**). Each TALEN monomer had a unique epitope tag and a mitochondrial localization sequence at the N terminus. The basic structure of the protein is shown in **Supplementary Figure 1a**. Western blots showed that proteins of the expected size were synthesized after transient transfection with plasmids coding for the monomers (**Supplementary Fig. 1b**). Likewise, immunocytochemistry showed that they colocalized with the mitochondrial marker Mitotracker (**Fig. 1c**). Within the transcriptional unit of each mitoTALEN monomer, we added a fluorescent marker so that transfected cells could be sorted by FACS, with mCherry for the left monomer and eGFP for the right monomer (**Fig 1b**).

We tested the Δ5-mitoTALEN in human osteosarcoma cells heteroplasmic for the mtDNA common deletion (BH10.9 cells)[13] by transfecting them simultaneously with two independent plasmids, each coding for one Δ5-mitoTALEN monomer. Two days after transfection, cells were sorted by FACS gating for mCherry ('red') and eGFP ('green') expression (**Fig. 1d**). Cells expressing both markers, termed 'yellow', were expected to express both Δ5-mitoTALEN monomers. We also isolated cells not expressing any fluorescent markers ('black') and cells expressing only eGFP ('green'). Yields of cells expressing only mCherry were too low to permit analysis.

We analyzed mtDNA heteroplasmy with a three-primer PCR technique (Online Methods) using the primers depicted in **Figure 1a**. This analysis showed that the Δ5-mitoTALEN was effective in reducing the mtDNA deletion load and changing mtDNA heteroplasmy to a predominance of wild-type mtDNA (**Fig. 1e,f**). We then measured the levels of the different mtDNA species by quantitative PCR (qPCR) and found that the change in heteroplasmy was primarily caused by a reduction in the absolute levels of deletion-mutant mtDNA (**Supplementary Fig. 2**). There was a trend toward a reduction in the total mtDNA levels after 2 d, and we also observed a small reduction after 14 d (**Supplementary Fig. 2b,c**). However, we observed a significant compensatory increase in wild-type mtDNA levels at 14 d (**Supplementary Fig. 2**). Transfection with the Δ5-mitoTALEN in the homoplasmic parental osteosarcoma line (143B) did not change total mtDNA levels at either 2 or 14 d (**Supplementary Fig. 2b,c**), confirming the specificity of the-mitoTALEN.

We next tested the mitoTALEN approach against the Leber's hereditary optic neuropathy plus dystonia point mutation m.14459G>A in the *MT-ND6* gene[14]. Our rationale for the design of the 14459A-mitoTALEN was that the left monomer would bind the wild-type sequence adjacent to the mutation and that cleavage would be dictated by binding of the right monomer to a recognition sequence harboring m.14459A (**Fig. 2a**). A yeast single-strand annealing assay showed that the 14459A-mitoTALEN was able to differentially
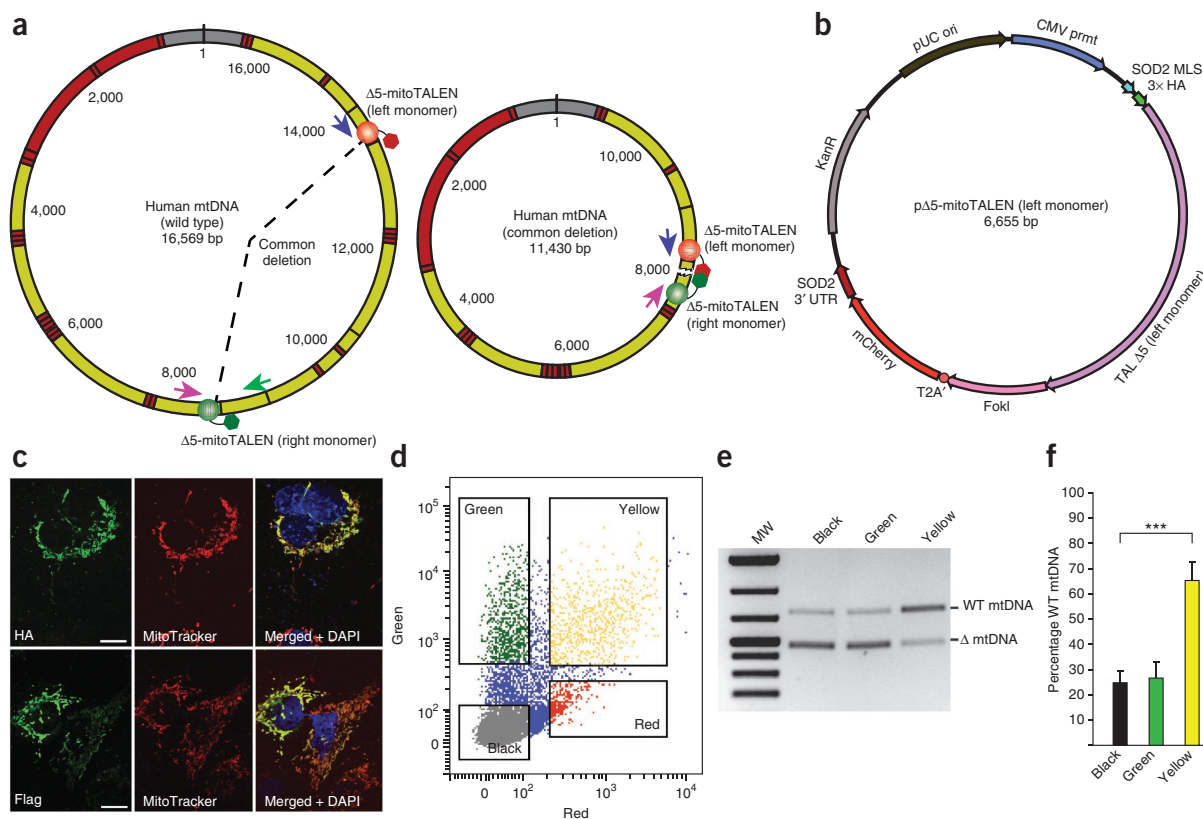
---

**Figure 1** Rationale, verification and efficacy of the Δ5-mitoTALEN for elimination of mtDNAs with the common deletion. (**a**) Diagram illustrating the location of each mitoTALEN monomer recognition site on wild-type mtDNA and mtDNA carrying the 'common deletion'. (**b**) Components of the plasmid used to express the mitoTALEN monomer linked to mCherry. A similar plasmid, not illustrated here, was used for the mitoTALEN monomer linked to eGFP. CMV prmt, cytomegalovirus promoter; SOD2 MLS, superoxide dismutase 2 mitochondrial localization signal; HA, hemagglutinin tag; TAL D5, TAL DNA binding domain; FokI, endonuclease domain; T2A, picornovirus translational stuttering sequence; SOD2 3′ UTR, 3′ untranslated region of the gene encoding SOD2; KanR, kanamycin resistance; pUC ori, plasmid origin of replication. (**c**) Verification of mitochondrial localization of Δ5-mitoTALEN monomers in COS-7 cells 24 h after transfection using antibodies against Flag or HA immuno-tags. Scale bars, 10 μm. (**d**) Gates used for cell sorting of eGFP ('Green') and mCherry ('Red') expression 48 h after transfection with plasmids for the Δ5-mitoTALEN monomers. Cell fractions that were not expressing fluorescent markers ('Black'), only one marker ('Green') and both eGFP and mCherry ('Yellow') were collected for analyses. (**e**) Three-primer PCR analysis to quantify the relative levels of deleted mtDNA, performed with the primers depicted by colored arrows in **a**. MW, molecular weight standard, 1,500–200 bp; WT, wild-type; Δ, deleted. (**f**) Quantification of three independent transfection experiments using three-primer PCR. Unpaired $t$-test between 'black' and 'yellow' values; $n = 3$; ***$P < 0.001$. Data are expressed as mean ± s.d.

cleave wild-type and mutant mtDNA sequences (**Supplementary Fig. 3**). We then re-engineered the construct and built the 14459A-mitoTALEN as described for the Δ5-mitoTALEN. Although nuclear pseudogenes of the *MT-ND6* gene exist, we did not detect a complete target site in the nuclear genome with the m.14459A sequence (**Supplementary Table 1**).

We tested the 14459A-mitoTALEN in two osteosarcoma cybrid lines harboring heteroplasmic amounts of the m.14459A mtDNA (clone 1 harboring 90% of m.14459A and clone 3 harboring 55% m.14459A). Transfections with the mitoTALEN were followed by FACS collection of 'black' and 'yellow' cells. Heteroplasmy analysis of amplicons spanning m.14459 showed that the mtDNA heteroplasmy once again shifted in the predicted direction with a marked increase in the relative abundance of wild-type mtDNA (**Fig. 2b,c**). The change was stable at 14 d after transfection (**Supplementary Fig. 4**), although at this time point we could not detect the mitoTALEN in the cells by western blot analysis (**Supplementary Fig. 5**). Analyses by qPCR showed that one of the tested clones (clone 1) had a transient decrease in total mtDNA levels, which is not surprising considering that it had close to 90% mutant mtDNA (**Fig. 2d**). However, this decrease was not observed after 14 d or in transfected parental 143B cells, which

indicates that the 14459A-mitoTALEN is specific for m.14459A and that the associated mtDNA depletion was due to the elimination of target mtDNA.

In contrast to the cells with heteroplasmic mtDNA deletions, which had enough wild-type genomes to show a normal biochemical phenotype, complex I activity was partially decreased in the clone with high levels of m.14459A mutant mtDNA (clone 1) (**Fig. 2e**). This partial defect (approximately 35–40% residual activity) was similar to the activity previously reported for cells with high levels (approximately 95%) of mtDNA harboring the mutation[14]. As expected, transfection with the 14459A-mitoTALEN not only reduced the mutant mtDNA load but also increased complex I activity (**Fig. 2e**).

Although this study is solely based on cybrid models and animal experimentation may be required to ensure the safety of mitoTALENs *in vivo*, our previous studies have shown that transient expression of recombinant endonuclease in mitochondria is well tolerated in mouse muscle[15], heart and liver[4]. As expected, a transient mtDNA depletion was observed, although mtDNA levels were rapidly normalized through a well-recognized, but yet uncharacterized, mtDNA copy number control mechanism[16,17]. Nevertheless, caution will have to be exercised in situations when the levels of the mtDNA haplotype
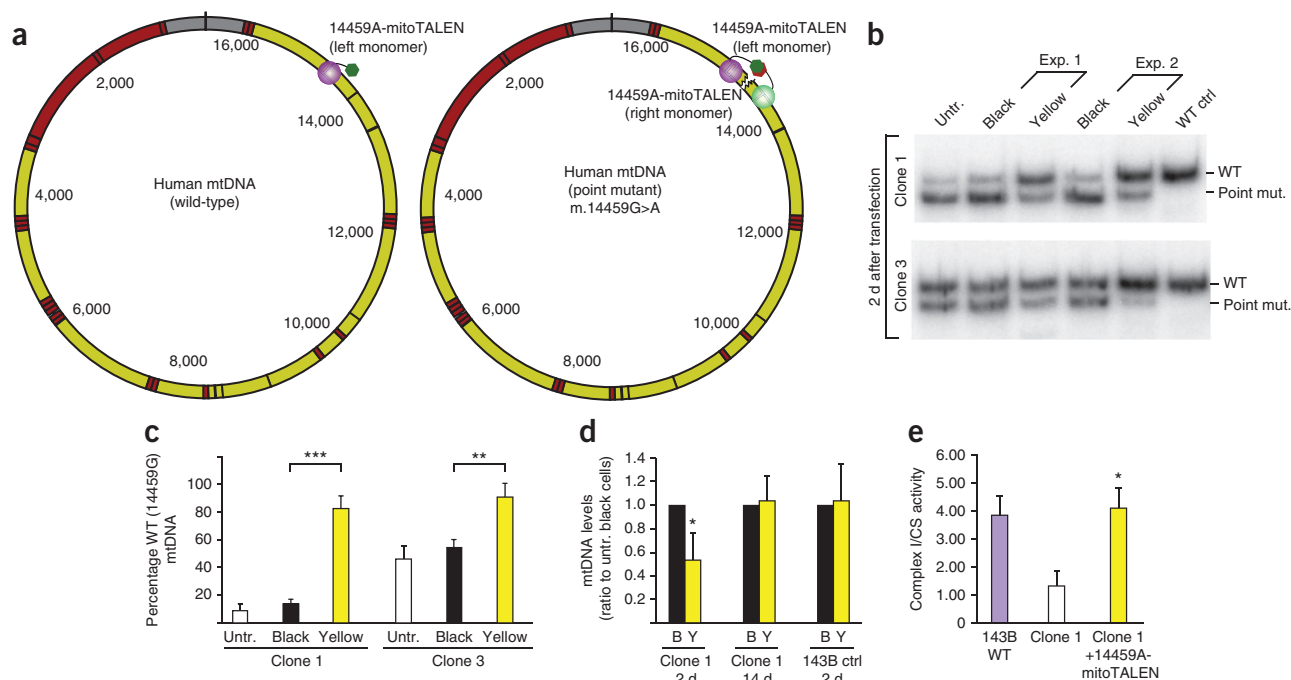
**Figure 2** Rationale and efficacy of the 14459A-mitoTALEN against the pathogenic m.14459A mtDNA point mutation. (**a**) Diagram illustrating the binding of 14459A-mitoTALEN monomers to wild-type mtDNA (left) or mutant mtDNA harboring the m.14459G>A point mutation (right). (**b**) Restriction-fragment length polymorphism (RFLP) analysis of the m.14459G>A load in cells 48 h after transfection and sorted by FACS with gating for 'black' and 'yellow' cell populations as in **Figure 1d** for the Δ5-mitoTALEN. WT, wild-type; Ctrl, control; Untr., untransfected cells; Exp. 1, Experiment 1; Exp. 2, Experiment 2. (**c**) Quantification of three independent experiments for each clone is shown. Untr., untransfected cells. (**d**) Quantification of the total mtDNA levels by qPCR showed a decrease in clone 1 at 2 d after transfection, but not at 14 d. Likewise, wild-type control 143B cells did not show a decrease in mtDNA levels after 2 d. B, black; Y, yellow. (**e**) Enzyme activity (complex I/citrate synthase (CS) ratio) in control cells, mutant cells and mutant cells transfected with the 14459A-mitoTALEN at 14 d after transfection. Unpaired $t$-test between 'black' and 'yellow' values; $n = 3$; $*P < 0.005$, $**P < 0.002$, $***P < 0.001$. Data are expressed as mean ± s.d.

targeted for elimination are close to 100%, as mtDNAs that carry mutations may contribute to the functional mitochondrial gene pool in some cases.

The delivery of therapeutic genes and proteins remains a barrier to the fast implementation of genetic therapies, particularly if they are large, as TALENs are. However, it is important to keep in mind that in comparison to gene therapy of the nuclear genome, where life-long expression of the corrective factor is the goal, transient expression of mitoTALENs should be sufficient to produce lasting changes in mtDNA heteroplasmy[4,15]. It is therefore reasonable to expect that permanent correction of heteroplasmy levels, potentially rescuing the oxidative phosphorylation deficiency in affected tissues, might be achieved after one or a small number of administrations of mito-TALEN, either as a genetic or protein agent.

## METHODS
Methods and any associated references are available in the online version of the paper.

*Note: Any Supplementary Information and Source Data files are available in the online version of the paper.*

### AUTHOR CONTRIBUTIONS
S.R.B. and S.L.W. designed and conducted most experiments and assisted in writing the manuscript. M.P. assisted in the quantification of mtDNA deletions and in writing the manuscript. S.P. conducted the complex I activity experiments and assisted in writing the manuscript. C.T.M. designed and supervised the project and wrote the manuscript.

### COMPETING FINANCIAL INTERESTS
The authors declare no competing financial interests.

Reprints and permissions information is available online at http://www.nature.com/reprints/index.html.

1. Schon, E.A., DiMauro, S. & Hirano, M. *Nat. Rev. Genet.* **13**, 878–890 (2012).
2. Vafai, S.B. & Mootha, V.K. *Nature* **491**, 374–383 (2012).
3. Wallace, D.C. *Environ. Mol. Mutagen.* **51**, 440–450 (2010).
4. Bacman, S.R., Williams, S.L., Garcia, S. & Moraes, C.T. *Gene Ther.* **17**, 713–720 (2010).
5. Comte, C. *et al. Nucleic Acids Res.* **41**, 418–433 (2013).
6. Taylor, R.W., Chinnery, P.F., Turnbull, D.M. & Lightowlers, R.N. *Nat. Genet.* **15**, 212–215 (1997).
7. Minczuk, M., Papworth, M.A., Miller, J.C., Murphy, M.P. & Klug, A. *Nucleic Acids Res.* **36**, 3926–3938 (2008).
8. Hockemeyer, D. *et al. Nat. Biotechnol.* **29**, 731–734 (2011).
9. Sung, Y.H. *et al. Nat. Biotechnol.* **31**, 23–24 (2013).
10. Schon, E.A. *et al. Science* **244**, 346–349 (1989).
11. Corral-Debrinski, M. *et al. Nat. Genet.* **2**, 324–329 (1992).
12. Soong, N.W., Hinton, D.R., Cortopassi, G. & Arnheim, N. *Nat. Genet.* **2**, 318–323 (1992).
13. Diaz, F. *et al. Nucleic Acids Res.* **30**, 4626–4633 (2002).
14. Jun, A.S., Trounce, I.A., Brown, M.D., Shoffner, J.M. & Wallace, D.C. *Mol. Cell Biol.* **16**, 771–777 (1996).
15. Bacman, S.R., Williams, S.L., Duan, D. & Moraes, C.T. *Gene Ther.* **19**, 1101–1106 (2012).
16. Carling, P.J., Cree, L.M. & Chinnery, P.F. *Mitochondrion* **11**, 686–692 (2011).
17. Moraes, C.T. *Trends Genet.* **17**, 199–205 (2001).

# ONLINE METHODS

**MitoTALEN construct.** Custom-made TALE domains were developed by Cellectis bioresearch according to the mtDNA sequence provided by the authors. The TALEN binds the following mtDNA sequences (TALE binding site underlined). The TALE-domain amino acid sequences are also listed.

*Common deletion breakpoint (Δ5-mitoTALEN).* AAAAT<u>ATTAAACACAAACT</u><u>AC</u>CACCTACCTCCCTCACC<u>ATTGGCAGCCTAGCA</u>TTAG.

*Left Δ5 TALE domain.* DIADLRTLGYSQQQQEKIKPKVRSTVAQHHEALVG HGFTHAHIVALSQHPAALGTVAVKYQDMIAALPEATHEAIVGVGKQWSG ARALEALLTVAGELRGPPLQLDTGQLLKIAKRGGVTAVEAVHAWRNALTG APLNLTPEQVVAIASNIGGKQALETVQALLPVLCQAHGLTPQQVVAIASNG GGKQALETVQRLLPVLCQAHGLTPEQVVAIASNIGGKQALETVQRLLPV LCQAHGLTPEQVVAIASNIGGKQALETVQALLPVLCQAHGLTPEQVVAIAS NIGGKQALETVQALLPVLCQAHGLTPEQVVAIASNIGGKQALETVQALLP VLCQAHGLTPEQVVAIASHDGGKQALETVQRLLPVLCQAHGLTPEQVVA IASNIGGKQALETVQALLPVLCQAHGLTPEQVVAIASHDGGKQALETVQR LLPVLCQAHGLTPEQVVAIASNIGGKQALETVQALLPVLCQAHGLTPEQV VAIASNIGGKQALETVQALLPVLCQAHGLTPEQVVAIASNIGGKQALETVQ ALLPVLCQAHGLTPEQVVAIASHDGGKQALETVQRLLPVLCQAHGLTPQ QVVAIASNGGGKQALETVQRLLPVLCQAHGLTPEQVVAIASNIGGKQALE TVQALLPVLCQAHGLTPQQVVAIASNGGGRPALESIVAQLSRPDPALAALT NDHLVALACLGGRPALDAVKKGLG.

*Right Δ5 TALE domain.* DIADLRTLGYSQQQQEKIKPKVRSTVAQHHEALVG HGFTHAHIVALSQHPAALGTVAVKYQDMIAALPEATHEAIVGVGKQWSG ARALEALLTVAGELRGPPLQLDTGQLLKIAKRGGVTAVEAVHAWRNALTG APLNLTPQQVVAIASNNGGKQALETVQRLLPVLCQAHGLTPEQVVAIASH DGGKQALETVQRLLPVLCQAHGLTPQQVVAIASNGGGKQALETVQRLLP VLCQAHGLTPEQVVAIASNIGGKQALETVQALLPVLCQAHGLTPQQVVAI ASNNGGKQALETVQRLLPVLCQAHGLTPQQVVAIASNNGGKQALETVQR LLPVLCQAHGLTPEQVVAIASHDGGKQALETVQRLLPVLCQAHGLTPQQ VVAIASNGGGKQALETVQRLLPVLCQAHGLTPQQVVAIASNNGGKQALE TVQRLLPVLCQAHGLTPEQVVAIASHDGGKQALETVQRLLPVLCQAHGL TPEQVVAIASHDGGKQALETVQRLLPVLCQAHGLTPEQVVAIASNIGGKQ ALETVQALLPVLCQAHGLTPEQVVAIASNIGGKQALETVQALLPVLCQAH GLTPQQVVAIASNGGGKQALETVQRLLPVLCQAHGLTPQQVVAIASNNG GKQALETVQRLLPVLCQAHGLTPQQVVAIASNGGGRPALESIVAQLSRPDP ALAALTNDHLVALACLGGRPALDAVKKGLG.

*Point-mutant m.14459A (14459A mitoTALEN).* CCCC<u>TGACCCCCATG</u>CCT CAGGATACTCCT<u>CAATAGCCATCa</u>CTGTA.

*Left (m.14459A TALE domain).* DIADLRTLGYSQQQQEKIKPKVRSTVAQHH EALVGHGFTHAHIVALSQHPAALGTVAVKYQDMIAALPEATHEAIVGVGK QWSGARALEALLTVAGELRGPPLQLDTGQLLKIAKRGGVTAVEAVHAWR NALTGAPLNLTPQQVVAIASNNGGKQALETVQRLLPVLCQAHGLTPEQV VAIASNIGGKQALETVQALLPVLCQAHGLTPEQVVAIASHDGGKQALETV QRLLPVLCQAHGLTPEQVVAIASHDGGKQALETVQRLLPVLCQAHGLTPE QVVAIASHDGGKQALETVQRLLPVLCQAHGLTPEQVVAIASHDGGKQAL ETVQRLLPVLCQAHGLTPEQVVAIASHDGGKQALETVQRLLPVLCQAHG LTPEQVVAIASNIGGKQALETVQALLPVLCQAHGLTPQQVVAIASNGGGK QALETVQRLLPVLCQAHGLTPQQVVAIASNGGGRPALESIVAQLSRPDPAL AALTNDHLVALACLGGRPALDAVKKGLG.

*Right (m.14459A TALE domain).* DIADLRTLGYSQQQQEKIKPKVRSTVAQ HHEALVGHGFTHAHIVALSQHPAALGTVAVKYQDMIAALPEATHEAIVG VGKQWSGARALEALLTVAGELRGPPLQLDTGQLLKIAKRGGVTAVEAVH AWRNALTGAPLNLTPQQVVAIASNNGGKQALETVQRLLPVLCQAHGLTP EQVVAIASNIGGKQALETVQALLPVLCQAHGLTPQQVVAIASNGGGKQAL ETVQRLLPVLCQAHGLTPQQVVAIASNNGGKQALETVQRLLPVLCQAHG LTPQQVVAIASNNGGKQALETVQRLLPVLCQAHGLTPEQVVAIASHDGG KQALETVQRLLPVLCQAHGLTPQQVVAIASNGGGKQALETVQRLLPVLC QAHGLTPEQVVAIASNIGGKQALETVQALLPVLCQAHGLTPQQVVAIASN GGGKQALETVQRLLPVLCQAHGLTPQQVVAIASNGGGKQALETVQRLLP

VLCQAHGLTPQQVVAIASNGGGRPALESIVAQLSRPDPALAALTNDHLVAL ACLGGRPALDAVKKGLG.

We modified plasmid constructs for mitoTALEN monomers using the In-Fusion HD cloning kit from Clontech Laboratories. Modifications included removal of the stock nuclear localization signal, inclusion of a mitochondrial localization signal derived from *SOD2* or *COX8A*, inclusion of a unique immuno-tag in the N terminus of the mature protein (hemagglutinin (HA) or Flag), inclusion of a 3′ untranslated region from a mitochondrial gene known to localize mRNA to ribosomes on mitochondria, inclusion of an independent fluorescent marker to select for expression (eGFP in one monomer and mCherry in the other) and inclusion of a recoded picornaviral 2A-like sequence (T2A′) between the mitoTALEN and the fluorescent marker[18]. In addition to using the two plasmids for cotransfection (**Fig. 1**), both left and right monomers were fused in a tandem plasmid as shown in **Supplementary Figure 6a**. This single plasmid produced more 'yellow' cells after sorting (**Supplementary Fig. 6b**), although changes in heteroplasmy were identical whether two plasmids or the combined one were used (data not shown).

**Single-strand annealing assay.** Single-strand annealing in *Saccharomyces cerevisiae* was performed as previously described[19].

**Cells, transfection and sorting.** Heteroplasmic cybrids harboring the 'common deletion' were derived from fusions of an osteosarcoma cell line devoid of mtDNA (143B/206 line[20]) and dermal fibroblasts from a patient harboring the common deletion, m.8483_13459del4977 (refs. 13,21). The research use of these non-identifiable cells was approved by the Columbia University Institutional Animal Care and Use Committee (IACUC) after patient informed consent. We used clone BH10.9, which was previously characterized[13]. Cybrid clones for the point-mutation model were derived in a similar way, by fusing dermal fibroblasts from a patient harboring the heteroplasmic missense mutation m.14459A in *MT-ND6* with 143B/206 cells[22] and manually picking and screening colonies for heteroplasmy levels of m.14459A. The research use of these non-identifiable cells was approved by the Columbia University IACUC after patient consent. The m.14459A point mutation has been reported and characterized in other patients[14,23]. Cells were transfected with GenJet DNA *In Vitro* Transfection Reagent version II (SL100489; SignaGen Laboratories) following the protocol suggested by the manufacturers. After 48 h, cells were sorted using a FACSAria IIU by gating on single-cell fluorescence using a 561-nm laser and 600LP, 610/20 filter set for mCherry and a 488-nm laser and 505LP, 530/30 filter set for eGFP.

**Western blot.** We subjected 40 μg of total proteins from cellular homogenates of COS 7 cells collected 48 h after transfection to electrophoresis in 4–20% Tris-HCl polyacrylamide gels (4561094; Bio-Rad Laboratories) and transferred the separated proteins to nitrocellulose membranes (162-0115, Bio-Rad), as described[4]. Antibodies used for blotting were rat monoclonal antibody to HA (1867423; Roche Biochemical; 1:1,000), mouse monoclonal antibody to Flag (F3165; Sigma-Aldrich; 1:1,000) and mouse monoclonal antibody to tubulin (T9026; Sigma-Aldrich; 1:1,000). Secondary antibodies were IRDye 800–conjugated antibody to rat IgG (612-732-120; 1:5,000), IRDye 800–conjugated antibody to mouse IgG (610-732-124; 1:5,000) and IRDye 700–conjugated antibody to mouse IgG (610-430-002; 1:5,000) from Rockland. An Odyssey Infrared Imaging System (LI-COR) was used to scan the blots.

**Immunocytochemical studies.** We plated COS-7 cells onto coverslips and then transfected them with mitoTALEN plasmids as above. At 24 h post transfection cells were incubated for 30 min at 37 °C with 200 nM MitoTracker Red CMXRos (Invitrogen) and fixed with 2% paraformaldehyde in PBS for 20 min. After a brief treatment with methanol (5 min), primary antibodies to HA (Roche; 1:200) or Flag (Sigma-Aldrich; 1:200) in 2% BSA in PBS were incubated overnight at 4 °C in a humid chamber. The next day, coverslips were incubated for 2 h at room temperature with Alexa Fluor 488–conjugated goat antibody to rat IgG (A-11006; Molecular Probes; 1:200) or Alexa Fluor 488–conjugated goat antibody to mouse IgG (A-11001; Molecular Probes; 1:200), as previously described[4]. Images were recorded using a Zeiss LSM510 confocal microscope.

**DNA extraction.** We extracted total DNA from FACS sorted cells with the NucleoSpin Tissue XS kit (740901.50; Macherey-Nagel, Clontech) according to the manufacturer's instructions.

**Three-primer PCR to quantify the ratios of deleted/wild-type molecules.** We applied this three-primer PCR approach as previously described[21]. Primers included F-m.8273_8289, B1-m.9028_9008 and B2-m.13720_13705, numbered relative to the human mtDNA reference NC_012920. Primer B1 corresponds to an mtDNA region inside the common deletion, whereas primers F and B2 flank the deleted region. Primers F and B1 only amplify wild-type mtDNAs, and primers F and B2 amplify Δ-mtDNAs. PCR products were cleaned using spin columns (740609.250; Macherey-Nagel, Clontech) and quantified with a Bioanalyzer system (Bioanalyzer 2100; Agilent).

**Quantification of m.14459A by 'last-cycle hot' PCR and RFLP.** We determined the levels of the m.14459G>A mutation by 'last-cycle hot' PCR[24,25], which visualizes only nascent amplicons and removes interference from point mutation heteroduplexes formed during melting and annealing cycles. Total DNA extracted from sorted cells was used as template, and PCR was performed with the following mtDNA primers, in which the mutant allele m.14459A completes a BclI half-site allowing restriction-fragment length polymorphism: F-BclI-mut-F, 5′-CCCCCATGCCTCAGGATACTCCTCAATAGTGATC-3′ and 14579B, 5′-TGATTGTTAGCGGTGTGGTCGGGTGTGT-3′. PCR products were digested with BclI and resolved in a 12% polyacrylamide gel. Radioactive signal was quantified using a Cyclone phosphorimaging system (PerkinElmer) and OptiQuant software (PerkinElmer).

**Quantitative PCR.** We performed quantitative PCR reactions using SYBR/ROX chemistry (172-5264; Bio-Rad, SsoAdvanced SYBR Green)[15] on a Bio-Rad CFX96/C1000 qPCR machine using the manufacturer's software to calculate $\Delta\Delta C_T$ values. We determined the levels of different mtDNA species between sorted cell populations by quantifying the levels of deletion breakpoint/actin, wild-type/actin and total mtDNA/actin. We used the primers below.

Inside the common deletion (detects only wild-type mtDNA): 8537F: 5′-ATCTGTTCGCTTCATTCATTGC-3″ and 8661B: 5′-GGTGGTGATTA GTCGGTTGT-3′.

Breakpoint of the common deletion (detects only Δ5-deleted mtDNA): 8410F: 5′-CATACTCCTTACACTATTCCTCAT-3′ and 13479B: 5′-TGCTAATGCT AGGCTGCCA-3′.

Outside the common deletion (detects total mtDNA): 12s rRNA-F: 5′-CTCACCACCTCTTGCTCAG-3′, 12s rRNA-B: 5′-GGCTACACCTTGACC

TAACG-3′, Cytb-F: 5′-AATCACCACAGGACTATT-3′ and Cytb-B: 5′-GTA GGAAGAGGCAGATAA-3′.

Nuclear DNA primers: β-actin exon 6-F: 5′-GCGCAAGTACTCTGTGTGGA-3′ and β-actin exon 6-B: 5′-CATCGTACTCCTGCT-3′.

**Search for mitoTALEN target sequences in the nuclear genome.** We created a BLAST database containing all the chromosomes from HG19 (GRCh37.p4) except mtDNA (chrM) using CLCBio Genomics Workbench. This was aligned with complete mitoTALEN target sites, including spacer sequence, to create a list of similar sequences. We screened each list using a motif search algorithm to count identical occurrences of individual mitoTALEN monomer recognition sites.

**Enzyme activities.** For spectrophotometric analysis, we subjected $2.5 \times 10^7$ exponentially growing cells to centrifugation and washed them once with PBS. The pellets were resuspended in 1 ml of 10 mM HEPES buffer (pH 7.4), 0.5 mM EDTA, 0.5 mM EGTA and 250 mM sucrose and then sonicated twice in ice-cold water for 10 s with 30 s intervals. To eliminate cellular debris, samples were centrifuged at 500*g*, and the supernatant was used as reaction sample for spectrometric analysis as previously described[26]. Complex I (NADH CoQ oxidoreductase) reaction was started with coenzyme Q1 (100 μM) and inhibited with rotenone (10 μM). Citrate synthase reaction was started with oxaloacetate (0.5 mM). Assay results were normalized to protein concentration obtained by the Bradford method (Bio-Rad), and subsequently complex I activity was normalized to citrate synthase activity. Assays were performed in a BioTek Synergy H1 hybrid plate reader.

**Statistical analyses.** Pairwise comparisons were performed using two-tailed Student's *t*-test using Excel software (Microsoft). Data is expressed as mean ± s.d.

18. Szymczak, A.L. *et al. Nat. Biotechnol.* **22**, 589–594 (2004).
19. Liddell, L., Manthey, G., Pannunzio, N. & Bailis, A. *J. Vis. Exp.* e3150 http://dx.doi.org/10.3791/3150 (2011).
20. King, M.P. & Attardi, G. *Science* **246**, 500–503 (1989).
21. Sciacco, M., Bonilla, E., Schon, E.A., DiMauro, S. & Moraes, C.T. *Hum. Mol. Genet.* **3**, 13–19 (1994).
22. Bacman, S.R. & Moraes, C.T. *Methods Cell Biol.* **80**, 503–524 (2007).
23. Jun, A.S., Brown, M.D. & Wallace, D.C. *Proc. Natl. Acad. Sci. USA* **91**, 6206–6210 (1994).
24. Bayona-Bafaluy, M.P., Blits, B., Battersby, B.J., Shoubridge, E.A. & Moraes, C.T. *Proc. Natl. Acad. Sci. USA* **102**, 14392–14397 (2005).
25. Moraes, C.T., Ricci, E., Bonilla, E., DiMauro, S. & Schon, E.A. *Am. J. Hum. Genet.* **50**, 934–949 (1992).
26. Martinez, B. *et al. J. Neurochem.* **78**, 1054–1063 (2001).